

M e GOLDEN L I E p o t e n s e n n e d o u g h t
t o e n c e n c e b y p o o t i s t o t c o s u e

X L ¹⁺ ID, L ¹⁺ S obo We ¹ ID Yu u G o ¹ Ho u Pe ¹ ID Rud u Ge ¹ ID Zefu Lu ¹ ID
Pe W u We u Z ou ^{1*} ID

1. Institute of Crop Sciences, Chinese Academy of Agricultural Sciences, Beijing 100081, China

2020 C. S. Center for Excellence in Molecular Plant Sciences, Institute of Plant Physiology and Ecology, Chinese Academy of Sciences, Shanghai 200032, China

* author for correspondence: hou.enb@n.cas.cn

[†]These authors contributed equally.

The author responsible for distribution of materials integral to the findings presented in this article in accordance with the policy described in the instructions for authors: <https://academic.oup.com/plphys/pages/general-instructions> Wenbin Zhou: zhouwenbin@caas.cn.

Abstract

Drought stress becomes one of the most severe abiotic stresses experienced in agricultural production across the world. Plants respond to water deficit via stomatal movements in the leaves, which are mainly regulated by abscisic acid (ABA). Previous study from our lab showed that constitutive expression of maize *ZmGLK1* (OLDEN-1; L. E. L.) transcription factors in rice *Oryza sativa* L. can improve stomatal conductance and plant photosynthetic capacity under field conditions. In the present study, we uncovered a function of *ZmGLK1* regulation of stomatal movement in rice during drought stress. We found that elevated drought tolerance in rice plants overexpressing *ZmGLK1* or *GOLDEN2* (*ZmGLK2*) is conferred by rapid ABA-mediated stomatal closure. Comparative analysis of RNA-sequencing (RNA-seq) data from their coleoptyles and DNase-seq by purification sequencing (DPS) results obtained *in vitro* revealed that *ZmGLK1* played roles in regulating ABA-related and stress response pathways. Four upregulated genes closely functioning in abiotic stress tolerance with strong binding peaks in the DPS data were identified as putative target genes of *ZmGLK1* and *ZmGLK2* in rice. These results demonstrated that maize *GLK* plays an important role in regulating stomatal movements to coordinate photosynthesis and stress tolerance. This trait is a valuable target for breeding drought-tolerant crop plants without compromising photosynthetic capacity.

Introduction

Global crop production must be approximately doubled by 2050 to meet the demands of the increasing human population (F. O. 2009; Timlin et al. 2011). However, yield improvement has stagnated in recent years and is clearly projected to fall short of the expected demand (Ray et al. 2013). Yield stagnation in major crops is caused by a combination of factors including climate change, soil erosion, and cultivar restriction (Ray et al. 2011). Drought is one of the most severe natural hazards in agricultural production; it has affected large agricultural areas and been exacerbated by global de-

over the last 50 yr. **F O 0 1**. Rice (*Oryza sativa* L.) serves as a staple food for nearly half of the world's population, but it is a high water consuming crop and is particularly susceptible to drought. Over 50% of the world's rice production is estimated to be affected by drought stress **mb y x am et al 2 017**. Development of low water consuming and drought tolerant rice varieties is urgently needed to meet global food demand under changing climatic conditions **Tod s et al 2 017**.

Stomata are the main channels for the exchange between plants and the atmosphere. When plants suffer from water

Received: August 27, 2013; accepted: September 19, 2013; online access publication: October 18, 2013.

© The author(s) 2013. Published by Oxford University Press on behalf of American Society of Plant Biologists.

This is an Open Access article distributed under the terms of the Creative Commons Attribution License (<https://creativecommons.org/licenses/by/4.0/>), which permits unrestricted reuse, distribution, and reproduction in any medium, provided the original work is properly cited.

Open Access

deficit or are exposed to other environmental stimuli (e.g., low light intensity, low air humidity, high CO₂ levels, and pathogens), stomata are rapidly closed, especially in the epidermis (Seel et al. 2018). This dynamic movement is driven by turgor pressure changes in the guard cells, as a result of the activation of anion channels and the inhibition of K⁺ outward rectifying K⁺ channels, which encoded by K⁺ CHANNEL IN ARABIDOPSIS THALIANA KAT and ARABIDOPSIS K⁺ TRANSPORTER AKT genes (Munier et al. 2010). The efflux of anions and small metabolites, including Cl⁻, NO₃⁻, and malate, causes membrane depolarization to activate the outward rectifying K⁺ channel and Cl⁻ efflux, further reducing turgor pressure inside the guard cells and leading to the stomatal closure (Pridmore et al. 2007). Under water deficit conditions, the phytohormone abscisic acid (ABA) plays as the primary regulator of stomatal movement to prevent water loss, in which endogenous ABA levels are controlled by a precise balance between biosynthesis and catabolism, which also influenced by transport and conjugation process (Munier et al. 2010; Hsu et al. 2011). ABA is biologically synthesized from G₀ carotenoids to form xanthophylls (e.g., *cis*-violaxanthin and *cis*-neoxanthin); a C₁₅ intermediate, xanthoxin, is formed in the plastids via oxidative cleavage catalyzed by *cis*-epoxycarotenoid dioxygenase (NCED). Xanthoxin is then exported to the cytosol and converted to ABA through a 2-step reaction via short-chain dehydrogenase/reductase 1 (SDR1/BA1) and rice *OsDREHYDROXYLASE3* (O3) (Seo and Yoshida 2000; Ouyang and Zhang 2003).

Transcription factors (TFs) are crucial regulators of many biological processes, including responses to environmental signals and hormone regulation. These regulatory functions are accomplished through binding to specific *cis* elements in the promoter regions of target genes (Tordella et al. 2019). Numerous abiotic stress responsive TFs have been identified in plants; for instance, WRKY, MYB, and DREB/CBF TFs have all been reported as key regulators of plant stress responses (Munier et al. 2011). OLDEN-LIKE 1 (OLD1) TFs generally act as transcriptional activators of chloroplast development and biogenesis (Ross et al. 2001; Wang et al. 2013) and play important roles in regulating nuclear photosynthesis-related genes (Chen et al. 2016). In maize *Zea mays* L., *ZmGLK* genes, *ZmGLK1* and *GOLDEN2* (*ZmGLK2*), have shown differential expression patterns between mesophyll cells and the bundle sheath (Hill et al. 1998; Chang et al. 2019). Ectopic overexpression of maize *GLK* genes in rice induces chloroplast development in bundle sheath cells and activates intercellular plasmodesmal connections, considering the key step in forming intermedial protostoma in the transition from C₃ to C₄ photosynthesis (Wang et al. 2017). In a previous study from our lab, we showed that constitutive *ZmGLK* expression in rice leads to increased xanthophyll content and further mitigates the photo-inhibition under high light conditions, resulting in enhanced photosynthetic capacity with higher stomatal conductance and improved biomass and grain yield in the field (Liu et al. 2020). Moreover, *ZmGLK* also function in abiotic stress responses (Munier et al. 2010) and pathogen resistance

(Munier et al. 2010); for example, *ZmGLK* affects stomatal movement in rice *Oryza sativa* L. when exposed to drought (Nagesh et al. 2016).

In this study, we uncovered the dual function of maize *ZmGLK* and the ectopic overexpression of *ZmGLK1* and *ZmGLK2* in rice conferred improved drought tolerance by promoting stomatal closure in response to water deficit while maintaining high stomatal conductance to obtain efficient photosynthesis when sufficient water is available. We further showed that rapid stomatal movement was mediated by ABA-involved pathway under drought conditions. These results suggest that *GLK* genes may be promising candidates for breeding rice varieties with high stomatal flexibility and sustainable yield, which could strongly improve agricultural production and increase food security in the context of climate change.

Results

ZmGLK1 and *ZmGLK2* conferred improved drought tolerance in rice

In our previous study, *OsDREHYDROXYLASE3* rice lines constitutively expressing *ZmGLK1* or *ZmGLK2* driven by the maize *Ubiquitin* (*ZmUBI*) promoter performed improved photosynthesis rates and higher stomatal conductance (Liu et al. 2020). We further explored the stomatal responses of transgenic rice plants to water deficit in pot experiments in the growth chamber. Surprisingly, transgenic rice plants exhibited stronger drought tolerance than the wild-type (WT) plants after recovery from a 10 d drought treatment (Fig. 1). Specifically, the survival rates of *ZmUBI_{pro}:ZmGLK1* and *ZmUBI_{pro}:ZmGLK2* plants were 53.0% to 67.0% after the 6 d recovery period, which were significantly higher than the WT (17.3%; Fig. 1B). Moreover, the relative water content (RWC) in the leaves of WT and transgenic plants ranged from 67.7% to 85.3% before drought but decreased to 73.1% in the WT after water was withheld for 7 d. In comparison, *ZmUBI_{pro}:ZmGLK1* and *ZmUBI_{pro}:ZmGLK2* plants maintained relatively high RWC, especially *ZmUBI_{pro}:ZmGLK2*, ranging from 86.9% to 90.9%. After 10 d of drought stress, the RWC values of WT and *ZmUBI_{pro}:ZmGLK1* plants decreased to 11.6% to 19.9%, which were significantly lower than those of *ZmUBI_{pro}:ZmGLK2* plants (17.5% to 18.6%; Fig. 1C). These results indicated that *ZmGLK1* and *ZmGLK2* both conferred higher capacities for water conservation and thus drought tolerance.

We next tested the growth performance of WT, *ZmUBI_{pro}:ZmGLK1*, and *ZmUBI_{pro}:ZmGLK2* rice plants to PE-induced osmotic stress as a drought simulation. After growth in 0% PE (6000) for 10 d, *ZmUBI_{pro}:ZmGLK1* and *ZmUBI_{pro}:ZmGLK2* rice plants showed less wilting and chlorosis compared to the WT (Supplemental Fig. S1). The maximum quantum efficiency of photosystem II (PSII) (F_v/F_m) as measured as an important indicator of plant physiological state under stress conditions, and the F_v/F_m

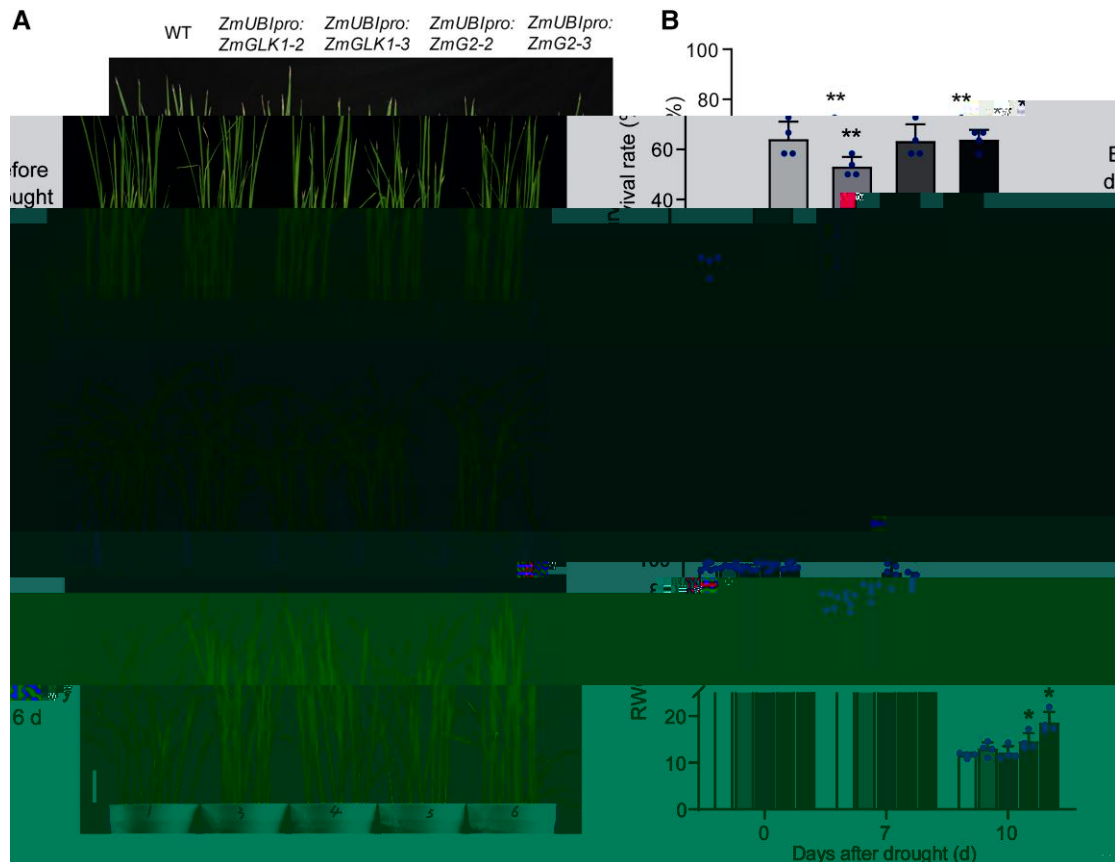


Figure 1. Overexpression of *ZmGLK1* and *ZmG2* in rice increased drought tolerance. **A)** Phenotypes of WT, *ZmUBI_{pro}:ZmGLK1*, and *ZmUBI_{pro}:ZmG2* rice plants during drought stress. Three-week-old WT, *ZmUBI_{pro}:ZmGLK1*, and *ZmUBI_{pro}:ZmG2* rice seedlings grown in soil were drought stressed by withholding water for 10 d and then watered for a 6 d recovery period. The upper, middle, and lower panels show representative plants before drought stress, after 10 d of drought stress, and after the 6 d recovery, respectively. Scale bar = 1 cm. **B)** Survival rates of WT, *ZmUBI_{pro}:ZmGLK1*, and *ZmUBI_{pro}:ZmG2* rice plants after 10 d of drought stress followed by 6 d of recovery. Data are presented as the mean \pm SD from 3 biological replicates. **C)** The RWC of WT, *ZmUBI_{pro}:ZmGLK1*, and *ZmUBI_{pro}:ZmG2* rice leaves after 0, 7, and 10 d of drought stress. Data are presented as the mean \pm SD from 3 biological replicates. **P* < 0.05, ***P* < 0.01, ****P* < 0.001.

10 d of PE treatment (Supplemental Fig. S1B). We also monitored changes of RWC in rice seedlings during PE treatment. The results showed that the transgenic plants retained significantly higher RWC compared to the WT. Specifically, RWC values were 11.4% to 11.1% and 9.5% to 9.7% higher in *ZmUBI_{pro}:ZmGLK1* and *ZmUBI_{pro}:ZmG2* rice plants, respectively, compared to the WT (Supplemental Fig. S1C). These results together indicated that overexpression of *ZmGLK1* and *ZmG2* in rice significantly improve the tolerance to drought and osmotic stress.

ZmGLK1 and ZmG2 gene expression and drought stress response

To further investigate the physiological mechanism underlying the elevated drought tolerance conferred by *ZmGLK1* and *ZmG2*, we evaluated the effects of drought treatment on stomatal traits of rice seedlings grown in the pots in the growth chamber, since stomata are the main channels for gas exchange and water vapor in plants, serving as the dominant limitation to photosynthesis under drought. We therefore first measured

stomatal conductance and photosynthesis related parameters under control conditions using a LiCOR 6400 T portable photosynthesis system. The results revealed significantly higher stomatal conductance in *ZmUBI_{pro}:ZmGLK1* and *ZmUBI_{pro}:ZmG2* rice seedlings (0.118–0.130 and 0.106–0.131, respectively) compared to the WT (0.083) under control condition; while the transgenic plants also performed higher photosynthesis rates, intercellular CO₂ concentrations (C_i), and transpiration rates (Supplemental Fig. S2), as the plants grown in the field (Fig. 2A–C). In contrast, after 7 d of drought treatment, *ZmUBI_{pro}:ZmGLK1* and *ZmUBI_{pro}:ZmG2* rice plants displayed sharply decrease in stomatal conductance (0.06–0.073 and 0.057–0.059, respectively), whereas that of WT remained relatively stable under drought conditions (0.087; Supplemental Fig. S2B). The photosynthesis rates, C_i, and transpiration rates showed corresponding declines in *ZmUBI_{pro}:ZmGLK1* and *ZmUBI_{pro}:ZmG2* rice plants during water deprivation (Supplemental Fig. S2, C, and D).

We next compared the stomatal traits between WT and *ZmUBI_{pro}:ZmGLK1* or *ZmUBI_{pro}:ZmG2* rice plants under

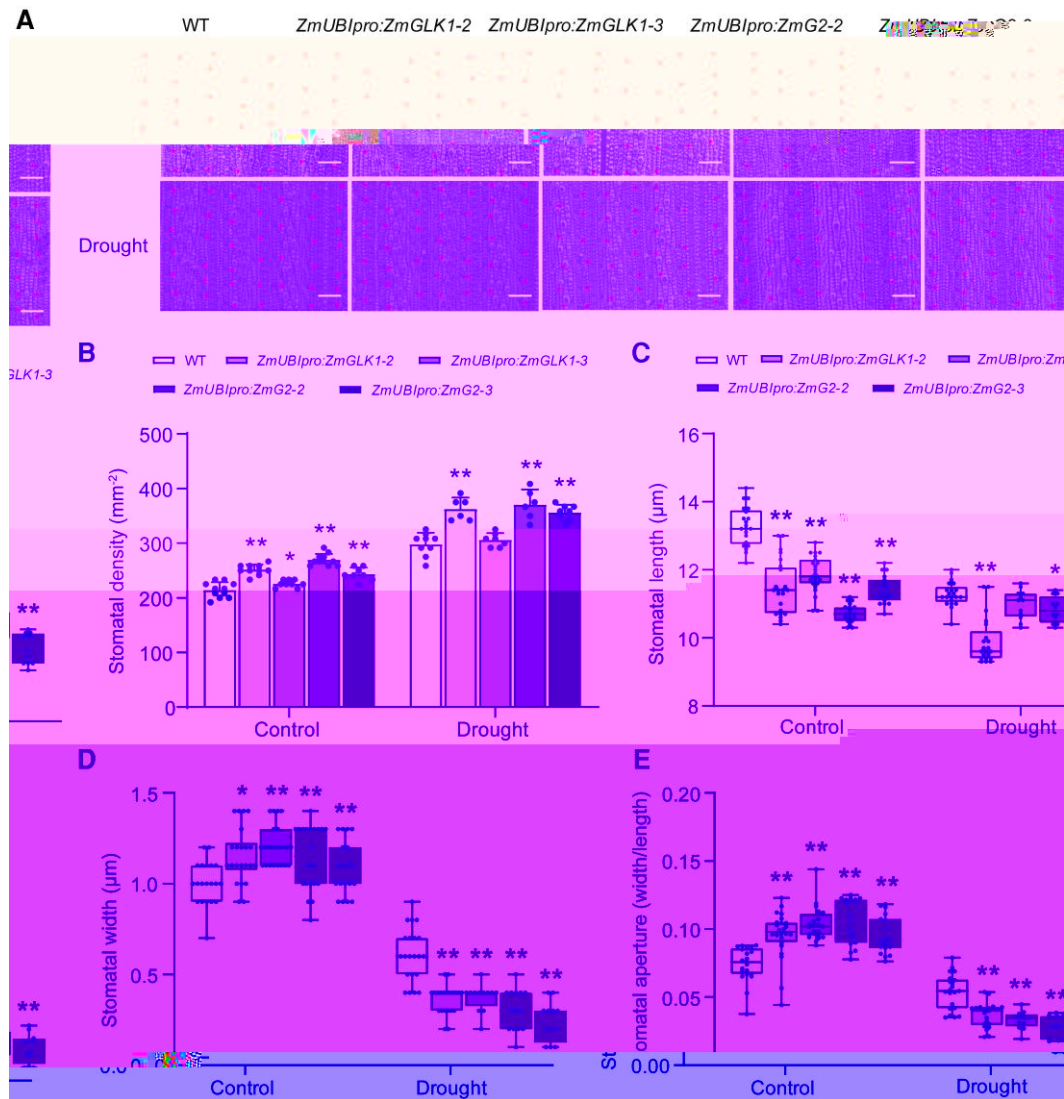


FIGURE 2 | ZmUBIpro:ZmGLK1 and ZmUBIpro:ZmG2 rice plants show higher stomatal density and lower stomatal aperture under drought conditions. (A) Micrographs of stomata for WT, ZmUBIpro:ZmGLK1-2, ZmUBIpro:ZmGLK1-3, ZmUBIpro:ZmG2-2, and ZmUBIpro:ZmG2-3 rice plants under Control and Drought conditions. (B) Stomatal density (mm^{-2}) for WT, ZmUBIpro:ZmGLK1-2, ZmUBIpro:ZmGLK1-3, ZmUBIpro:ZmG2-2, and ZmUBIpro:ZmG2-3 rice plants under Control and Drought conditions. (C) Stomatal length (μm) for WT, ZmUBIpro:ZmGLK1-2, ZmUBIpro:ZmGLK1-3, ZmUBIpro:ZmG2-2, and ZmUBIpro:ZmG2-3 rice plants under Control and Drought conditions. (D) Stomatal width (μm) for WT, ZmUBIpro:ZmGLK1-2, ZmUBIpro:ZmGLK1-3, ZmUBIpro:ZmG2-2, and ZmUBIpro:ZmG2-3 rice plants under Control and Drought conditions. (E) Stomatal aperture (width/length) for WT, ZmUBIpro:ZmGLK1-2, ZmUBIpro:ZmGLK1-3, ZmUBIpro:ZmG2-2, and ZmUBIpro:ZmG2-3 rice plants under Control and Drought conditions. Significance levels are indicated by asterisks (*, **).

both control and drought conditions. Transgenic plants presented higher stomatal density in the leaves but had significantly shorter stomata compared to the WT regardless of conditions (Fig. 2B, C). Intriguingly, the stomata were prominently wider in ZmUBIpro:ZmGLK1 and ZmUBIpro:ZmG2 rice leaves compared to the WT under control conditions (Fig. 2D), whereas under drought stress, the stomatal widths were significantly decreased in transgenic plants to a lower level than WT, consistent with the stomatal aperture data (Fig. 2E).

Considering the relative low light intensity in the growth chamber could lead to the stomatal closure, we further conducted an experiment in the greenhouse. In this natural light to exclude the influence of low light, as expected, the results

showed consistency with the chamber experiment (Fig. 1).

All plants were severely impaired due to the rapid loss of water during the 10 d drought duration (Supplemental Fig. S3; Fig. 3A). After re-watering for 7 d, we observed the higher survival rate in ZmUBIpro:ZmGLK1 and ZmUBIpro:ZmG2 rice plants (Fig. 3B), as well as the significantly higher RWC of leaves than WT either during the drought or the recovery stage (Fig. 3C). Moreover, we monitored the dynamics of photosynthesis rate and stomatal conductance throughout the duration of drought, and that ZmUBIpro:ZmGLK1 and ZmUBIpro:ZmG2 rice plants performed higher photosynthesis rate and stomatal conductance under sufficient water condition. Nevertheless, the photosynthesis rate and stomatal conductance of all plants were generally declined as the

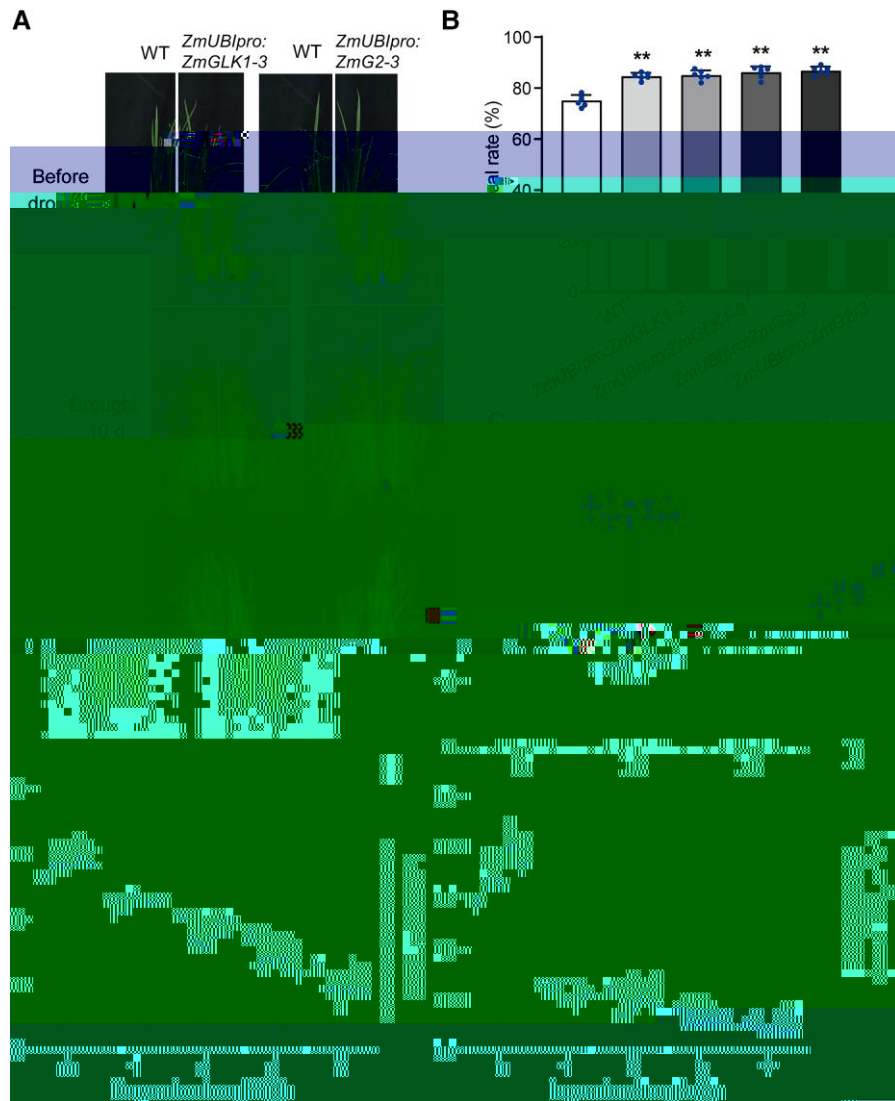


Figure 3. ZmGLK1 confers rapid stomatal closure to prevent water loss in rice during drought. **A)** Phenotypes of WT, ZmUBI_{pro}:ZmGLK1, and ZmUBI_{pro}:ZmG2 rice plants during drought stress. Sixty-day-old WT, ZmUBI_{pro}:ZmGLK1, and ZmUBI_{pro}:ZmG2 rice plants grown in soil in the greenhouse. The drought-stressed plants were held in water for 10 d and then transferred for a 7 d recovery period. The upper, middle, and lower panels show representative plants before drought stress, after 10 d of drought stress, and after the 7 d of recovery, respectively. Scale bar: 10 cm. **B)** Survival rates of WT, ZmUBI_{pro}:ZmGLK1, and ZmUBI_{pro}:ZmG2 rice plants after 10 d of drought stress followed by 7 d of recovery. **C)** The RWC of WT, ZmUBI_{pro}:ZmGLK1, and ZmUBI_{pro}:ZmG2 rice leaves after 0 and 7 d of drought stress and after 7 d of recovery. **D, E)** Dynamic change of photosynthesis rate (**D**) and stomatal conductance (**E**) of WT, ZmUBI_{pro}:ZmGLK1, and ZmUBI_{pro}:ZmG2 rice plants during the drought stress. Data are presented as the mean \pm SD from 3 to 6 biological replicates. * $P < 0.05$, ** $P < 0.01$ (Student's *t* test).

drought deepened, of which ZmUBI_{pro}:ZmGLK1 and ZmUBI_{pro}:ZmG2 rice plants presented lower photosynthesis rate and the stomatal conductance compared to the WT (Fig. 3, D and E). These results together clearly indicated that the rapid stomatal closure was triggered by water deficiency in ZmUBI_{pro}:ZmGLK1 and ZmUBI_{pro}:ZmG2 rice plants, further contributing to the elevated drought tolerance.

Regulation of photosynthesis and stomatal movement by ABA in ZmUBI_{pro}:ZmGLK1 and ZmUBI_{pro}:ZmG2 rice plants
During the drought stress, ABA is the pivotal phytohormone that regulates stomatal movement to respond drought

Chen et al. 2020. To further dissect the underlying mechanism associated with stomatal movement induced by ZmGLK1 and ZmG2, exogenous rice plants that B to clarify whether the rapid stomatal closure was B induced. After 15 h of applying 100 μ M B, ZmUBI_{pro}:ZmGLK1 and ZmUBI_{pro}:ZmG2 rice plants showed strongly decreased photosynthesis rates, accompanied with the reduced stomatal conductance (Fig. 4, A and B). Accordingly, the C_i and transpiration rate were generally lower in ZmUBI_{pro}:ZmGLK1 and ZmUBI_{pro}:ZmG2 rice plants compared with the WT after B application (Fig. 4, C and D). The effects of exogenous B application on photosynthetic traits and stomatal conductance in

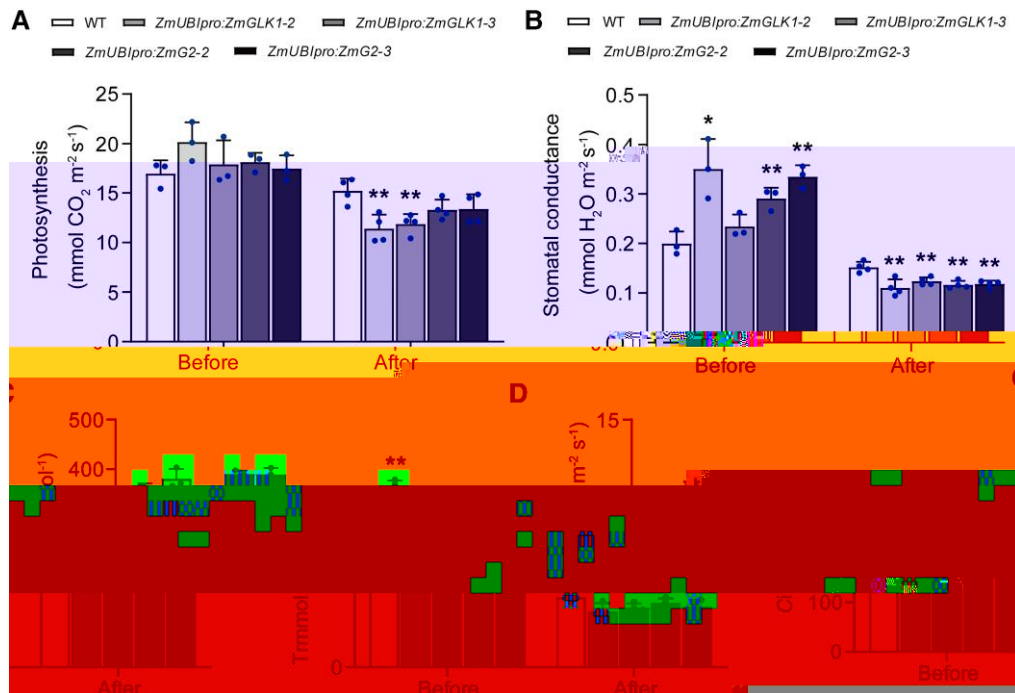


Figure 4. Exogenous B application reduced the photosynthesis rate and stomatal conductance in rice plants overexpressing ZmGLK1 or ZmG2 compared to the WT. **A)** Photosynthesis rates, **B)** stomatal conductance, **C)** C, and **D)** transpiration rates of 3-week-old WT, ZmUBIpro:ZmGLK1, and ZmUBIpro:ZmG2 rice plants grown in soil before or 15 h after B treatment. Data are shown as the mean \pm SD from 3 biological replicates. * $P < 0.05$, ** $P < 0.01$. Student's *t* test.

the WT and transgenic plants mimicked the results obtained from the drought stress treatments, which indicated the regulation of rapid stomatal closure in response to water deficit stress conferred by ZmGLK1 and ZmG2 as B mediated.

ZmGLK1 and ZmG2 regulate stomatal movement

To further understand the molecular mechanisms regulated by ZmGLKs under drought stress, we next compared the expression levels of several genes associated with stomatal movement in WT, ZmUBIpro:ZmGLK1, and ZmUBIpro:ZmG2 rice plants under control and drought stress conditions.

Under control conditions, several key genes were highly expressed in the transgenic plants compared to the WT but profoundly downregulated in response to drought stress. These comprised genes encoding proteins associated with guard cell signaling, such as *OsKAT5* and *OsAKT1* gene, 1 *TPase*, *OsAHA7*, and several stress response genes including *OsbZIP23*, *OsP5CS1*, and *OsLEA3* (Fig. 5). These results demonstrated that ZmGLK1 and ZmG2 improved drought tolerance by downregulating genes involved in stomatal movement when suffering from water deficit.

Genome-wide transcriptomic analysis was also conducted in WT, ZmUBIpro:ZmGLK1, and ZmUBIpro:ZmG2 rice plants at 3 h after B treatment to investigate the global effects of ZmGLK1 and ZmG2 introduced by B, especially

on stomatal movement. WT plants clearly showed distinct expression patterns compared to ZmUBIpro:ZmGLK1 and ZmUBIpro:ZmG2 plants, as demonstrated by the clear separation of the principal component analysis (PCA) (Fig. 6). Specifically, after B treatment, 70 and 775 genes were significantly upregulated in ZmUBIpro:ZmGLK1 and ZmUBIpro:ZmG2 plants, respectively, compared to the WT, of which 48 genes were upregulated in both transgenic lines (Fig. 6B).

Gene Ontology (GO) term enrichment analysis revealed that the upregulated differentially expressed genes (DEGs) in ZmUBIpro:ZmGLK1 and ZmUBIpro:ZmG2 plants functioned in multiple biological processes but primarily in the B and water deprivation pathways (Fig. 6, C and D). Next, we performed DNase-seq by purification sequencing (DPS) analysis to identify genes directly regulated by the ZmGLK1 TFs. This analysis revealed 6,601 and 6,565 putative binding sites of ZmGLK1 and ZmG2 in the rice genome, respectively,

with more than half of the identified sites being bound by both ZmGLK1 and ZmG2 (Supplemental Fig. S9). Of the 3,835 binding sites shared by ZmGLK1 and ZmG2, 17.44% were located to promoters, 8.59% to exons, and 5.6% to intergenic regions (Supplemental Fig. S9B). Motif analysis demonstrated that the most enriched core motifs found in the ZmGLK1 and ZmG2 binding regions were CCTCT and TTCT (Supplemental Fig. S9, C and D). Fifty-nine genes

identified from the DPS data as potential targets of ZmGLK1 and ZmG2 in rice were also identified from the RNA-seq data as differentially expressed

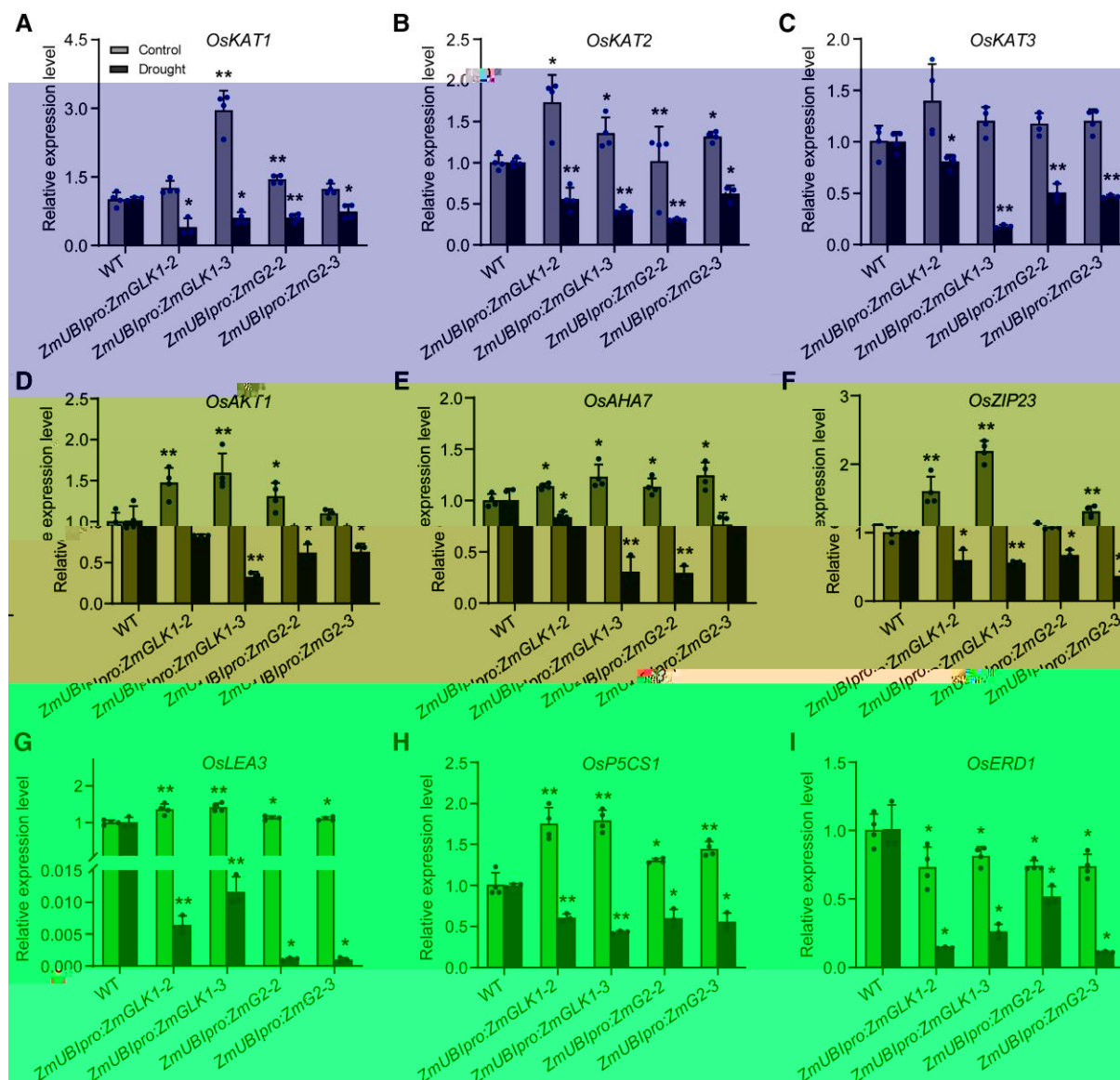


Figure 5. Relative expression levels of genes involved in stomatal movement and stomatal aperture in WT, ZmUBIpro:ZmGLK1, and ZmUBIpro:ZmG2 rice under normal conditions and after 7 d of drought stress. Expression levels of **A)** *OsKAT1*, **B)** *OsKAT2*, **C)** *OsKAT3*, **D)** *OsAKT1*, **E)** *OsAHA7*, **F)** *OsZIP23*, **G)** *OsLEA3*, **H)** *OsP5CS1*, and **I)** *OsERD1*. Gene expression levels were measured by RT-qPCR in the leaves of 3-week-old rice plants grown in soil under normal conditions or drought stress for 7 d. Data are presented as the mean \pm SD from 3 biological replicates. * $P < 0.05$, ** $P < 0.01$ Student's *t* test.

in plants overexpressing ZmGLK1 or ZmG2 (Fig. 6B; Supplemental Table S1). We noticed upregulated DEs are annotated to abiotic stress tolerance and showed strong binding peaks in the D-P seq analysis simultaneously. Therefore, these genes were identified as putative target genes of ZmL1 and Zm2 in rice, including rice genes *Filamentation Temperature Sensitive Protein H6* (*OsFtsH6*), *Cytochrome P450 Family 714 B1* (*OsCYP714B1*), *Red Chlorophyll Catabolite Reductase 1* (*OsRCCR1*), and *Subtilisin-like Protease 57* (*OsSub57*; Fig. 7, C to D). The gene expression from RNA-seq data of these genes is prominently higher in ZmUBIpro:ZmGLK1 and ZmUBIpro:ZmG2 rice plants (Fig. 7E to F). Further reverse transcription

quantitative PCR (RT-qPCR) analysis verified that these genes are highly induced in ZmUBIpro:ZmGLK1 and ZmUBIpro:ZmG2 rice under drought stress conditions (Fig. 7, G to L). These putative target genes may contribute to enhanced drought tolerance by enabling rapid stomatal movement when suffering from water deficit.

Discussion

LTs have long been regarded as some of the most important regulators of chloroplast biogenesis and photosynthetic organelle formation; they have been identified in various species, from *Solanum lycopersicum* L., and maize

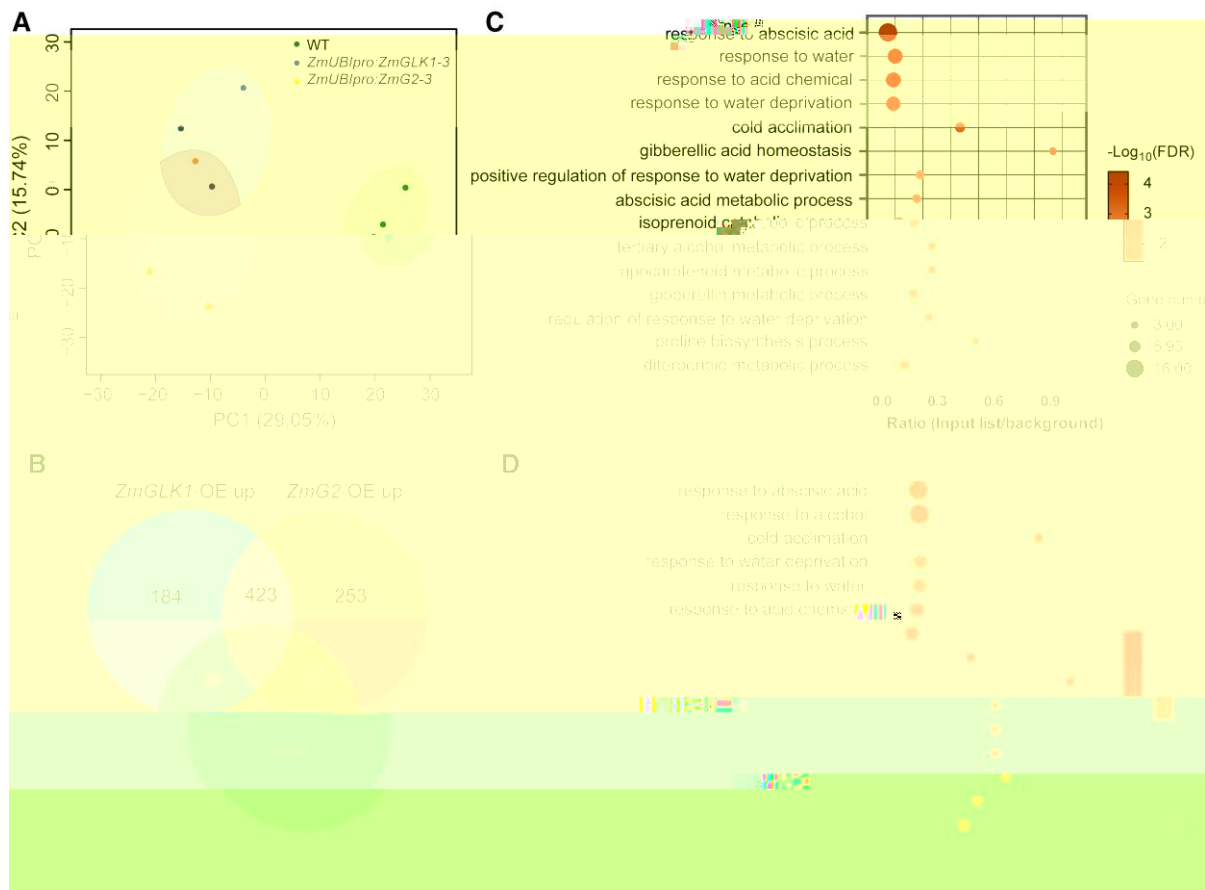


Figure 6. Transcriptomic analysis of WT, ZmUBI_{pro}:ZmGLK1, and ZmUBI_{pro}:ZmG2 rice plants at 3 h after B treatment. **A)** PC of gene expression in WT, ZmUBI_{pro}:ZmGLK1-3, and ZmUBI_{pro}:ZmG2-3 rice plants based on RNA-seq data. **B)** Venn diagram overlaid DEs upregulated in ZmUBI_{pro}:ZmGLK1 and ZmUBI_{pro}:ZmG2 rice plants compared to the WT and unique overlaid ZmGLK1 and ZmG2 target genes identified from DESeq. DEs were identified based on $|\log_2 \text{fold change}| > 1$ and $P < 0.05$ by DESeq R package. **C, D)** GO functional categories for DEs upregulated in ZmUBI_{pro}:ZmGLK1 **C)** and ZmUBI_{pro}:ZmG2 **D)** rice plants compared to the WT. Bubble size indicates the number of DE counts in the corresponding GO category; bubble intensity corresponds to the $-\log_{10}$ false discovery rate (FDR) value; and the X axis indicates the ratio of DEs in each GO category to all genes in the category.

Ross et al. 2001; Waters et al. 2009; Poell et al. 2011). In rice, ectopic expression of maize GLK genes (ZmGLK1) and ZmG2 promotes a prototrophic status in the leaf epidermis, increases chloroplast and mitochondrial development in rice vascular sheath cells (Wang et al. 2017). Previous study by our lab has revealed that rice plants overexpressing maize GLK genes have increased biomass and grain yield as a result of improved photosynthetic capacity and reduced photorespiration under high and fluctuating light conditions (Liu et al. 2020).

In the present study, we uncovered that overexpression of maize GLK genes (ZmGLK1 and ZmG2) in rice enhanced drought tolerance by promoting stomatal closure. Specifically, when plants were grown under standard, well-watered conditions, we observed smaller stomatal size but higher stomatal density and stomatal aperture in rice plants overexpressing ZmGLK1 or ZmG2 compared to the WT plants (Fig. 2, B and E). These results were consistent with earlier studies showing that ZmGLK1 and ZmG2 overexpression led

to increased stomatal conductance in *Arabidopsis* rice (Liu et al. 2020), greenhouse grown rice (Chen et al. 2022), and rice crops (Nagesh et al. 2016). In contrast, under drought stress, the stomata of ZmGLK1 or ZmG2 overexpressing rice plants rapidly closed (Fig. 2B and 3E), improving drought tolerance by preventing water loss. Previous studies in rice have reported that small, high density stomata can close quickly, thus promoting resilience against drought stress (Cane et al. 2019; Cane et al. 2023); these prior results were consistent with those of the present study. Notably, differences in stomatal status between control and drought-stressed plants as a result of ZmGLK1 or ZmG2 overexpression were directly caused by regulation of genes involved in stomatal movement, namely K^+ and Cl^- channels and H^+ ATPase (e.g., *OsKAT5*, *OsAKT1*, and *OsAHK7*; Fig. 5). Regulation of K^+ channel genes by ZmGLK1 or ZmG2 overexpression under normal conditions is unlike the previous study in rice crops showing that *ZmGLK1* is a positive regulator of K^+ channel genes and stomatal movement (Nagesh et al. 2016); thus, this rapid

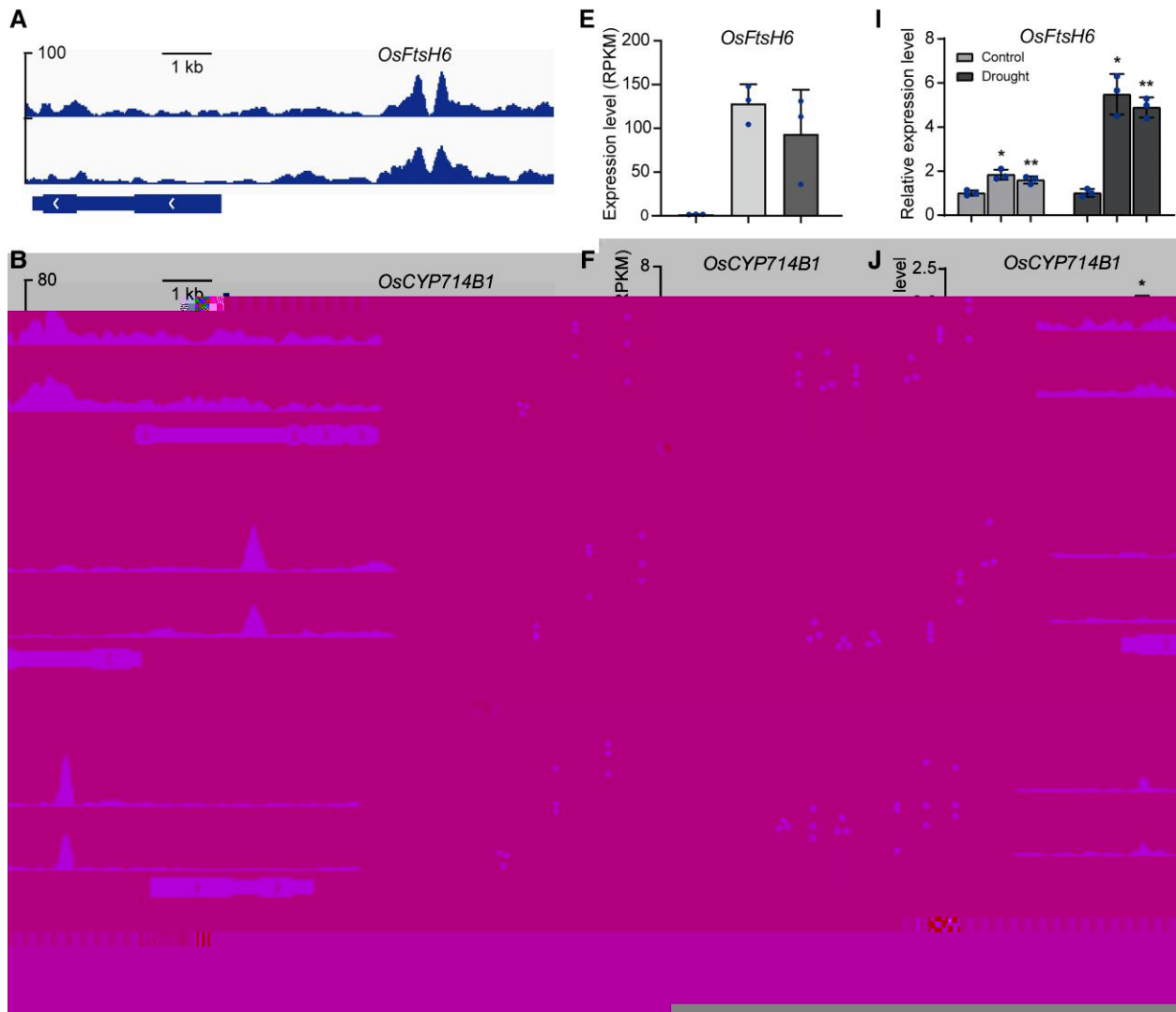


Figure 7. Putative Zm L1 and Zm L2 target genes in rice. **A to D)** ChIP-seq indicated that Zm L1 and Zm L2 preferentially bound to the promoters of *OsSub57A* (**A**), *OsFtsH6B* (**B**), *OsCYP714B1C* (**C**), and *OsRCCR4D* (**D**). **E to H)** Expression levels of *OsSub57E* (**E**), *OsFtsH6F* (**F**), *OsCYP714B1G* (**G**), and *OsRCCR4H* (**H**) in WT rice and rice overexpressing ZmGLK1 or ZmG2 as determined by RNA-seq analysis. Gene expression is calculated in RPKM. **I to L)** Relative expression levels of *OsSub57I* (**I**), *OsFtsH6J* (**J**), *OsCYP714B1K* (**K**), and *OsRCCR4L* (**L**) in WT, ZmUBIpro:ZmGLK1, and ZmUBIpro:ZmG2 rice under control conditions and after 7 d of drought stress as determined by RT-qPCR. Data are presented as the mean \pm SD from 3 biological replicates. * $P < 0.05$, ** $P < 0.01$. Student's *t* test.

stomatal closure of transgenic rice plants resulted directly from a significant reduction in the expression levels of those genes under drought conditions.

Notably, we verified that the regulation of rapid stomatal closure in response to water deficit is B-mediated, supported by the exogenous application of B inducing faster stomatal closure in ZmUBIpro:ZmGLK1 and ZmUBIpro:ZmG2 lines compared to the WT (Fig. 4B), which mimicked the effects of drought stress. Our findings are consistent with the previous study that suggested the fast stomatal closure requires a high B sensitivity (Candao Sobrinho et al. 2022). Our results also implied that Zm Ls may function in the B biosynthesis pathway, as indicated by the higher B accumulation (Supplemental Fig. S5) along with the abundant expression

of several key genes involved in B biosynthesis (e.g., *OsNCED2*, *OsNCED3*, *OsAAO3*, and *OsZEP1*) in response to drought (Supplemental Fig. S6). B biosynthesis starts with the epoxidation of xanthin and the xanthophyll precursor therefore plays an important role in B biosynthesis. We previously discovered that Zm Ls increase levels of xanthophylls, including xanthin and lutein (Liu et al. 2020), which may lead to the improved B biosynthesis in the leaf. Moreover, a study in Arabidopsis showed that Ls directly activate the expression of *WRKY40*, and L-WRKY40 together negatively regulates B signaling (Kim et al. 2019), suggesting a possible regulatory role of Zm Ls in the B signaling pathway. We also proposed that the G-like traits conferred by Zm Ls as mentioned above may contribute to the rapid stomatal

closure. This has been demonstrated by model simulations and experimental data that major C₃ crops are capable of more rapid stomatal closure compared to C₄ crops in response to water deficit, resulting in the high water use efficiency (WUE) (McAusland et al. 2016; Wang et al. 2011; Oke et al. 2012). Notably, previous studies have demonstrated that slower stomatal closure in ferns is associated with reduced responsiveness to B⁺ and sugars compared to angiosperms (Lima et al. 2019; Cárdeno Sobrino et al. 2017), whether rapid transport of ions and osmolytes between guard cells and subsidiary cells in grass species contributes to the fast stomatal movement (Chen et al. 2017). Rice plants overexpressing ZmGLKs have improved carbohydrate contents (Liu et al. 2010), consistent with SIGLK gene expression in tomato plants (Pelle et al. 2011; Nguyen et al. 2017); this may contribute to rapid stomatal closure at the metabolic level.

To further reveal the mechanism underlying Zm L-regulated stomatal movement, we conducted a comparative analysis of RNA-seq and DTP-seq data. This analysis revealed several potential target genes showing strong binding peaks, including *OsFtsH6*, *OsCYP714B1*, *OsRCCR1*, and *OsSub57* (Fig. 7). *OsFtsH6*, which belongs to the *OsFtsH* gene family, is involved in D1 turnover as part of the PS_{II} repair cycle. D1 turnover comprises removal of damaged D1 proteins by FtsH proteases located in the chloroplast, followed by coordinated assembly of newly synthesized D1 proteins into the thylakoid membrane (Wang et al. 2016). The high levels of D1 protein observed in ZmGLK1 and ZmG2 overexpressing plants in our previous study (Liu et al. 2010) prompted us to hypothesize the potential regulatory function of Zm Ls on *OsFtsH6* expression. *OsCYP714B1* encodes a bberellin 13-oxidase that plays a critical role in 13-hydroxylation to regulate plant growth (Mugome et al. 2013). *OsRCCR1* encodes a chlorophyll degradation enzyme; knocking down *OsRCCR1* leads to chlorotic lesions in older leaves and early senescence (Tang et al. 2011). Further, *OsSub57* is annotated as encoding a subtilisin homologue that is salt and drought induced (Liu et al. 2017; Zheng et al. 2012), but its function remains unknown. Nevertheless, it remains an open question whether the transcriptional regulation conferred by the heterologous gene is conserved or distinct from the native species, due to the complexity of gene regulatory system.

Stomatal closure is considered as the first reaction to drought stress in most plants, preventing water loss through transpiration, improving the ability of stomatal response as a feasible and effective strategy to maximize photosynthesis (Liu and Weng simultaneously; Li et al. 2019). It is worth noting that investigations into the functions of the potential target genes and regulatory roles as well as the quantitative analysis of stomatal kinetics of ZmGLK overexpressing plants are still needed to understand the mechanism by which Zm Ls fine-tune stomatal movements to coordinate trade-offs between photosynthesis and drought tolerance. Further exploration will provide insights and useful targets for crop breeding, enabling creation of elite varieties with both high photosynthetic capacity and drought tolerance.

Materials and methods

Plant growth conditions

The WT rice *O. sativa* spp. *japonica* cultivar *Itake* and homozygous lines described by Liu et al. (2010) ZmUBI_{pro}:ZmGLK1 and ZmUBI_{pro}:ZmG2 were used in this study. For hydroponic culture, rice seedlings were grown in modified Murashige-Skoog (MS) solution (0.5 mM NH₄⁺NO₃, 0.5 mM MgSO₄ · 7H₂O, 0.5 mM KNO₃, 0.5 mM CaCl₂ · 2H₂O, 0.5 mM KH₂PO₄, 0.5 mM NaH₂PO₄, 0.5 mM Na₂SiO₃ · 9H₂O, 0.5 mM FeCl₃ · 6H₂O, 0.5 mM MnCl₂ · 4H₂O, 0.5 mM ZnSO₄ · 7H₂O, 0.5 mM CuSO₄ · 5H₂O, 0.5 mM NiSO₄ · 6H₂O, 0.5 mM CoCl₂ · 6H₂O, 0.5 mM MoO₃ · 2H₂O, 0.5 mM B₂O₃ · 3H₂O, 0.5 mM H₃BO₃, 0.5 mM Na₂CO₃, 0.5 mM Na₂HPO₄ · 12H₂O, 0.5 mM NaH₂PO₄ · 12H₂O, 0.5 mM Na₂SO₄ · 10H₂O, 0.5 mM Na₂SiO₃ · 9H₂O, 0.5 mM Na₂CO₃ · 10H₂O, 0.5 mM Na₂HPO₄ · 12H₂O, 0.5 mM NaH₂PO₄ · 12H₂O, 0.5 mM Na₂SO₄ · 10H₂O, 0.5 mM Na₂SiO₃ · 9H₂O, 0.5 mM Na₂CO₃ · 10H₂O, 0.5 mM Na₂HPO₄ · 12H₂O, 0.5 mM NaH₂PO₄ · 12H₂O, 0.5 mM Na₂SO₄ · 10H₂O, 0.5 mM Na₂SiO₃ · 9H₂O, 0.5 mM Na₂CO₃ · 10H₂O, 0.5 mM Na₂HPO₄ · 12H₂O, 0.5 mM NaH₂PO₄ · 12H₂O, 0.5 mM Na₂SO₄ · 10H₂O, 0.5 mM Na₂SiO₃ · 9H₂O, 0.5 mM Na₂CO₃ · 10H₂O, 0.5 mM Na₂HPO₄ · 12H₂O, 0.5 mM NaH₂PO₄ · 12H₂O, 0.5 mM Na₂SO₄ · 10H₂O, 0.5 mM Na₂SiO₃ · 9H₂O, 0.5 mM Na₂CO₃ · 10H₂O, 0.5 mM Na₂HPO₄ · 12H₂O, 0.5 mM NaH₂PO₄ · 12H₂O, 0.5 mM Na₂SO₄ · 10H₂O, 0.5 mM Na₂SiO₃ · 9H₂O, 0.5 mM Na₂CO₃ · 10H₂O, 0.5 mM Na₂HPO₄ · 12H₂O, 0.5 mM NaH₂PO₄ · 12H₂O, 0.5 mM Na₂SO₄ · 10H₂O, 0.5 mM Na₂SiO₃ · 9H₂O, 0.5 mM Na₂CO₃ · 10H₂O, 0.5 mM Na₂HPO₄ · 12H₂O, 0.5 mM NaH₂PO₄ · 12H₂O, 0.5 mM Na₂SO₄ · 10H₂O, 0.5 mM Na₂SiO₃ · 9H₂O, 0.5 mM Na₂CO₃ · 10H₂O, 0.5 mM Na₂HPO₄ · 12H₂O, 0.5 mM NaH₂PO₄ · 12H₂O, 0.5 mM Na₂SO₄ · 10H₂O, 0.5 mM Na₂SiO₃ · 9H₂O, 0.5 mM Na₂CO₃ · 10H₂O, 0.5 mM Na₂HPO₄ · 12H₂O, 0.5 mM NaH₂PO₄ · 12H₂O, 0.5 mM Na₂SO₄ · 10H₂O, 0.5 mM Na₂SiO₃ · 9H₂O, 0.5 mM Na₂CO₃ · 10H₂O, 0.5 mM Na₂HPO₄ · 12H₂O, 0.5 mM NaH₂PO₄ · 12H₂O, 0.5 mM Na₂SO₄ · 10H₂O, 0.5 mM Na₂SiO₃ · 9H₂O, 0.5 mM Na₂CO₃ · 10H₂O, 0.5 mM Na₂HPO₄ · 12H₂O, 0.5 mM NaH₂PO₄ · 12H₂O, 0.5 mM Na₂SO₄ · 10H₂O, 0.5 mM Na₂SiO₃ · 9H₂O, 0.5 mM Na₂CO₃ · 10H₂O, 0.5 mM Na₂HPO₄ · 12H₂O, 0.5 mM NaH₂PO₄ · 12H₂O, 0.5 mM Na₂SO₄ · 10H₂O, 0.5 mM Na₂SiO₃ · 9H₂O, 0.5 mM Na₂CO₃ · 10H₂O, 0.5 mM Na₂HPO₄ · 12H₂O, 0.5 mM NaH₂PO₄ · 12H₂O, 0.5 mM Na₂SO₄ · 10H₂O, 0.5 mM Na₂SiO₃ · 9H₂O, 0.5 mM Na₂CO₃ · 10H₂O, 0.5 mM Na₂HPO₄ · 12H₂O, 0.5 mM NaH₂PO₄ · 12H₂O, 0.5 mM Na₂SO₄ · 10H₂O, 0.5 mM Na₂SiO₃ · 9H₂O, 0.5 mM Na₂CO₃ · 10H₂O, 0.5 mM Na₂HPO₄ · 12H₂O, 0.5 mM NaH₂PO₄ · 12H₂O, 0.5 mM Na₂SO₄ · 10H₂O, 0.5 mM Na₂SiO₃ · 9H₂O, 0.5 mM Na₂CO₃ · 10H₂O, 0.5 mM Na₂HPO₄ · 12H₂O, 0.5 mM NaH₂PO₄ · 12H₂O, 0.5 mM Na₂SO₄ · 10H₂O, 0.5 mM Na₂SiO₃ · 9H₂O, 0.5 mM Na₂CO₃ · 10H₂O, 0.5 mM Na₂HPO₄ · 12H₂O, 0.5 mM NaH₂PO₄ · 12H₂O, 0.5 mM Na₂SO₄ · 10H₂O, 0.5 mM Na₂SiO₃ · 9H₂O, 0.5 mM Na₂CO₃ · 10H₂O, 0.5 mM Na₂HPO₄ · 12H₂O, 0.5 mM NaH₂PO₄ · 12H₂O, 0.5 mM Na₂SO₄ · 10H₂O, 0.5 mM Na₂SiO₃ · 9H₂O, 0.5 mM Na₂CO₃ · 10H₂O, 0.5 mM Na₂HPO₄ · 12H₂O, 0.5 mM NaH₂PO₄ · 12H₂O, 0.5 mM Na₂SO₄ · 10H₂O, 0.5 mM Na₂SiO₃ · 9H₂O, 0.5 mM Na₂CO₃ · 10H₂O, 0.5 mM Na₂HPO₄ · 12H₂O, 0.5 mM NaH₂PO₄ · 12H₂O, 0.5 mM Na₂SO₄ · 10H₂O, 0.5 mM Na₂SiO₃ · 9H₂O, 0.5 mM Na₂CO₃ · 10H₂O, 0.5 mM Na₂HPO₄ · 12H₂O, 0.5 mM NaH₂PO₄ · 12H₂O, 0.5 mM Na₂SO₄ · 10H₂O, 0.5 mM Na₂SiO₃ · 9H₂O, 0.5 mM Na₂CO₃ · 10H₂O, 0.5 mM Na₂HPO₄ · 12H₂O, 0.5 mM NaH₂PO₄ · 12H₂O, 0.5 mM Na₂SO₄ · 10H₂O, 0.5 mM Na₂SiO₃ · 9H₂O, 0.5 mM Na₂CO₃ · 10H₂O, 0.5 mM Na₂HPO₄ · 12H₂O, 0.5 mM NaH₂PO₄ · 12H₂O, 0.5 mM Na₂SO₄ · 10H₂O, 0.5 mM Na₂SiO₃ · 9H₂O, 0.5 mM Na₂CO₃ · 10H₂O, 0.5 mM Na₂HPO₄ · 12H₂O, 0.5 mM NaH₂PO₄ · 12H₂O, 0.5 mM Na₂SO₄ · 10H₂O, 0.5 mM Na₂SiO₃ · 9H₂O, 0.5 mM Na₂CO₃ · 10H₂O, 0.5 mM Na₂HPO₄ · 12H₂O, 0.5 mM NaH₂PO₄ · 12H₂O, 0.5 mM Na₂SO₄ · 10H₂O, 0.5 mM Na₂SiO₃ · 9H₂O, 0.5 mM Na₂CO₃ · 10H₂O, 0.5 mM Na₂HPO₄ · 12H₂O, 0.5 mM NaH₂PO₄ · 12H₂O, 0.5 mM Na₂SO₄ · 10H₂O, 0.5 mM Na₂SiO₃ · 9H₂O, 0.5 mM Na₂CO₃ · 10H₂O, 0.5 mM Na₂HPO₄ · 12H₂O, 0.5 mM NaH₂PO₄ · 12H₂O, 0.5 mM Na₂SO₄ · 10H₂O, 0.5 mM Na₂SiO₃ · 9H₂O, 0.5 mM Na₂CO₃ · 10H₂O, 0.5 mM Na₂HPO₄ · 12H₂O, 0.5 mM NaH₂PO₄ · 12H₂O, 0.5 mM Na₂SO₄ · 10H₂O, 0.5 mM Na₂SiO₃ · 9H₂O, 0.5 mM Na₂CO₃ · 10H₂O, 0.5 mM Na₂HPO₄ · 12H₂O, 0.5 mM NaH₂PO₄ · 12H₂O, 0.5 mM Na₂SO₄ · 10H₂O, 0.5 mM Na₂SiO₃ · 9H₂O, 0.5 mM Na₂CO₃ · 10H₂O, 0.5 mM Na₂HPO₄ · 12H₂O, 0.5 mM NaH₂PO₄ · 12H₂O, 0.5 mM Na₂SO₄ · 10H₂O, 0.5 mM Na₂SiO₃ · 9H₂O, 0.5 mM Na₂CO₃ · 10H₂O, 0.5 mM Na₂HPO₄ · 12H₂O, 0.5 mM NaH₂PO₄ · 12H₂O, 0.5 mM Na₂SO₄ · 10H₂O, 0.5 mM Na₂SiO₃ · 9H₂O, 0.5 mM Na₂CO₃ · 10H₂O, 0.5 mM Na₂HPO₄ · 12H₂O, 0.5 mM NaH₂PO₄ · 12H₂O, 0.5 mM Na₂SO₄ · 10H₂O, 0.5 mM Na₂SiO₃ · 9H₂O, 0.5 mM Na₂CO₃ · 10H₂O, 0.5 mM Na₂HPO₄ · 12H₂O, 0.5 mM NaH₂PO₄ · 12H₂O, 0.5 mM Na₂SO₄ · 10H₂O, 0.5 mM Na₂SiO₃ · 9H₂O, 0.5 mM Na₂CO₃ · 10H₂O, 0.5 mM Na₂HPO₄ · 12H₂O, 0.5 mM NaH₂PO₄ · 12H₂O, 0.5 mM Na₂SO₄ · 10H₂O, 0.5 mM Na₂SiO₃ · 9H₂O, 0.5 mM Na₂CO₃ · 10H₂O, 0.5 mM Na₂HPO₄ · 12H₂O, 0.5 mM NaH₂PO₄ · 12H₂O, 0.5 mM Na₂SO₄ · 10H₂O, 0.5 mM Na₂SiO₃ · 9H₂O, 0.5 mM Na₂CO₃ · 10H₂O, 0.5 mM Na₂HPO₄ · 12H₂O, 0.5 mM NaH₂PO₄ · 12H₂O, 0.5 mM Na₂SO₄ · 10H₂O, 0.5 mM Na₂SiO₃ · 9H₂O, 0.5 mM Na₂CO₃ · 10H₂O, 0.5 mM Na₂HPO₄ · 12H₂O, 0.5 mM NaH₂PO₄ · 12H₂O, 0.5 mM Na₂SO₄ · 10H₂O, 0.5 mM Na₂SiO₃ · 9H₂O, 0.5 mM Na₂CO₃ · 10H₂O, 0.5 mM Na₂HPO₄ · 12H₂O, 0.5 mM NaH₂PO₄ · 12H₂O, 0.5 mM Na₂SO₄ · 10H₂O, 0.5 mM Na₂SiO₃ · 9H₂O, 0.5 mM Na₂CO₃ · 10H₂O, 0.5 mM Na₂HPO₄ · 12H₂O, 0.5 mM NaH₂PO₄ · 12H₂O, 0.5 mM Na₂SO₄ · 10H₂O, 0.5 mM Na₂SiO₃ · 9H₂O, 0.5 mM Na₂CO₃ · 10H₂O, 0.5 mM Na₂HPO₄ · 12H₂O, 0.5 mM NaH₂PO₄ · 12H₂O, 0.5 mM Na₂SO₄ · 10H₂O, 0.5 mM Na₂SiO₃ · 9H₂O, 0.5 mM Na₂CO₃ · 10H₂O, 0.5 mM Na₂HPO₄ · 12H₂O, 0.5 mM NaH₂PO₄ · 12H₂O, 0.5 mM Na₂SO₄ · 10H₂O, 0.5 mM Na₂SiO₃ · 9H₂O, 0.5 mM Na₂CO₃ · 10H₂O, 0.5 mM Na₂HPO₄ · 12H₂O, 0.5 mM NaH₂PO₄ · 12H₂O, 0.5 mM Na₂SO₄ · 10H₂O, 0.5 mM Na₂SiO₃ · 9H₂O, 0.5 mM Na₂CO₃ · 10H₂O, 0.5 mM Na₂HPO₄ · 12H₂O, 0.5 mM NaH₂PO₄ · 12H₂O, 0.5 mM Na₂SO₄ · 10H₂O, 0.5 mM Na₂SiO₃ · 9H₂O, 0.5 mM Na₂CO₃ · 10H₂O, 0.5 mM Na₂HPO₄ · 12H₂O, 0.5 mM NaH₂PO₄ · 12H₂O, 0.5 mM Na₂SO₄ · 10H₂O, 0.5 mM Na₂SiO₃ · 9H₂O, 0.5 mM Na₂CO₃ · 10H₂O, 0.5 mM Na₂HPO₄ · 12H₂O, 0.5 mM NaH₂PO₄ · 12H₂O, 0.5 mM Na₂SO₄ · 10H₂O, 0.5 mM Na₂SiO₃ · 9H₂O, 0.5 mM Na₂CO₃ · 10H₂O, 0.5 mM Na₂HPO₄ · 12H₂O, 0.5 mM NaH₂PO₄ · 12H₂O, 0.5 mM Na₂SO₄ · 10H₂O, 0.5 mM Na₂SiO₃ · 9H₂O, 0.5 mM Na₂CO₃ · 10H₂O, 0.5 mM Na₂HPO₄ · 12H₂O, 0.5 mM NaH₂PO₄ · 12H₂O, 0.5 mM Na₂SO₄ · 10H₂O, 0.5 mM Na₂SiO₃ · 9H₂O, 0.5 mM Na₂CO₃ · 10H₂O, 0.5 mM Na₂HPO₄ · 12H₂O, 0.5 mM NaH₂PO₄ · 12H₂O, 0.5 mM Na₂SO₄ · 10H₂O, 0.5 mM Na₂SiO₃ · 9H₂O, 0.5 mM Na₂CO₃ · 10H₂O, 0.5 mM Na₂HPO₄ · 12H₂O, 0.5 mM NaH₂PO₄ · 12H₂O, 0.5 mM Na₂SO₄ · 10H₂O, 0.5 mM Na₂SiO₃ · 9H₂O, 0.5 mM Na₂CO₃ · 10H₂O, 0.5 mM Na₂HPO₄ · 12H₂O, 0.5 mM NaH₂PO₄ · 12H₂O, 0.5 mM Na₂SO₄ · 10H₂O, 0.5 mM Na₂SiO₃ · 9H₂O, 0.5 mM Na₂CO₃ · 10H₂O, 0.5 mM Na₂HPO₄ · 12H₂O, 0.5 mM NaH₂PO₄ · 12H₂O, 0.5 mM Na₂SO₄ · 10H₂O, 0.5 mM Na₂SiO₃ · 9H₂O, 0.5 mM Na₂CO₃ · 10H₂O, 0.5 mM Na₂HPO₄ · 12H₂O, 0.5 mM NaH₂PO₄ · 12H₂O, 0.5 mM Na₂SO₄ · 10H₂O, 0.5 mM Na₂SiO₃ · 9H₂O, 0.5 mM Na₂CO₃ · 10H₂O, 0.5 mM Na₂HPO₄ · 12H₂O, 0.5 mM NaH₂PO₄ · 12H₂O, 0.5 mM Na₂SO₄ · 10H₂O, 0.5 mM Na₂SiO₃ · 9H₂O, 0.5 mM Na₂CO₃ · 10H₂O, 0.5 mM Na₂HPO₄ · 12H₂O, 0.5 mM NaH₂PO₄ · 12H₂O, 0.5 mM Na₂SO₄ · 10H₂O, 0.5 mM Na₂SiO₃ · 9H₂O, 0.5 mM Na₂CO₃ · 10H₂O, 0.5 mM Na₂HPO₄ · 12H₂O, 0.5 mM NaH₂PO₄ · 12H₂O, 0.5 mM Na₂SO₄ · 10H₂O, 0.5 mM Na₂SiO₃ · 9H₂O, 0.5 mM Na₂CO₃ · 10H₂O, 0.5 mM Na₂HPO₄ · 12H₂O, 0.5 mM NaH₂PO₄ · 12H₂O, 0.5 mM Na₂SO₄ · 10H₂O, 0.5 mM Na₂SiO₃ · 9H₂O, 0.5 mM Na₂CO₃ · 10H₂O, 0.5 mM Na₂HPO₄ · 12H₂O, 0.5 mM NaH₂PO₄ · 12H₂O, 0.5 mM Na₂SO₄ · 10H₂O, 0.5 mM Na₂SiO₃ · 9H₂O, 0.5 mM Na₂CO₃ · 10H₂O, 0.5 mM Na₂HPO₄ · 12H₂O, 0.5 mM NaH₂PO₄ · 12H₂O, 0.5 mM Na₂SO₄ · 10H₂O, 0.5 mM Na₂SiO₃ · 9H₂O, 0.5 mM Na₂CO₃ · 10H₂O, 0.5 mM Na₂HPO₄ · 12H₂O, 0.5 mM NaH₂PO₄ · 12H₂O, 0.5 mM Na₂SO₄ · 10H₂O, 0.5 mM Na₂SiO₃ · 9H₂O, 0.5 mM Na₂CO₃ · 10H₂O, 0.5 mM Na₂HPO₄ · 12H₂O, 0.5 mM NaH₂PO₄ · 12H₂O, 0.5 mM Na₂SO₄ · 10H₂O, 0.5 mM Na₂SiO₃ · 9H₂O, 0.5 mM Na₂CO₃ · 10H₂O, 0.5 mM Na₂HPO₄ · 12H₂O, 0.5 mM NaH₂PO₄ · 12H₂O, 0.5 mM Na₂SO₄ · 10H₂O, 0.5 mM Na₂SiO₃ · 9H₂O, 0.5 mM Na₂CO₃ · 10H₂O, 0.5 mM Na₂HPO₄ · 12H₂O, 0.5 mM NaH₂PO₄ · 12H₂O, 0.5 mM Na₂SO₄ · 10H₂O, 0.5 mM Na₂SiO₃ · 9H₂O, 0.5 mM Na

Scanning electron microscopy

Rice leaves were detached from control or drought-treated plants and immediately cut into 3 × 3 mm pieces, excluding the veins. Samples were directly fixed in 2.5% (v/v) glutaraldehyde in 0.1 M phosphate buffer, pH 7.0, and then fixed with 1% osmium tetroxide. After washing twice with 0.1 M phosphate buffer, samples were dehydrated gradually in an ethanol series (30%, 50%, 60%, 70%, 80%, 90%, and 100%) for 15 min each, followed by incubating in tertiary butanol for 35 min. Then, samples were dried using a critical point dryer, pasted on the sample stage, and then coated with gold. Stomata were observed and photographed using a S-8010 scanning electron microscope (Hitachi, Japan). The size, number, and aperture sizes of stomata were calculated using ImageJ software.

Quantification of endogenous ABA contents

The uppermost expanded leaves of control and drought-stressed rice seedlings were detached and flash frozen in liquid nitrogen. Ground samples (100 mg each) were extracted with an acetone:triethylamine solution containing an internal standard at 4°C overnight. Samples were centrifuged, and the resulting supernatant was extracted again. The combined extracts were purified on a C₁₈ silica column and dried with nitrogen gas. After resolving in methanol and passing through a 0.2-µm filter, ABA was quantified on a HPLC–tandem mass spectrometry (MS/MS) system as described by Lu et al. (2017).

Exogenous ABA treatment

Forty-day-old rice seedlings grown in pots were sprayed with 100 µM ABA solution containing 0.5% (v/v) Tween 20 as a surfactant until the leaves were moist. The volume of ABA solution applied was consistent between seedlings. Two days after treatment, as exchange parameters and stomatal traits were evaluated as described above.

RNA extraction and RT-qPCR

The uppermost fully expanded leaves were harvested from 3-week-old rice seedlings grown in pots under normal conditions or drought stress for 7 d. Samples were flash frozen in liquid nitrogen and ground to powder, and then total RNA was extracted with TRIzol reagent in nitrogen. RNA purity and quantity were evaluated using a NanoDrop 2000 spectrophotometer (Thermo Fisher Scientific, USA). After DNase treatment, cDNA was synthesized from 1 µg of total RNA per sample using the Revert-First Strand cDNA Synthesis kit (Thermo Fisher Scientific, USA). RT-qPCR was performed using a QOD SYBR Green mix with the ROX TO-BO on a B-Box QuantStudio 6 Flex instrument (Applied Biosystems, USA). Relative transcript levels were calculated with the $2^{-\Delta\Delta CT}$ method (Livak and Schmittgen, 2001) with three biological replicates for each treatment, using *OsActin* as the internal control. Primers are listed in Supplemental Table S1.

RNA-seq analysis

Three days after exogenous ABA treatment, leaves were collected from 3-week-old rice seedlings grown in pots. Total RNA was extracted with TRIzol reagent, and then RNA integrity was assessed with the Agilent 2100 Bioanalyzer (Agilent Technologies, USA). RNA-seq libraries were constructed from WT, *ZmUBI_{pro}:ZmGLK1-3*, and *ZmUBI_{pro}:ZmG2-3* rice plants using the TruSeq Stranded mRNA LT Sample Prep kit (Illumina, USA) with three biological replicates per line. The resulting libraries were sequenced on the Illumina HiSeq 2500 sequencing platform. After removing the adaptor sequences and low-quality reads, clean reads were mapped to the *O. sativa* cv. Nipponbare reference genome using HISAT2 (Kim et al., 2015) and Bowtie (Langmead et al., 2009). Gene expression levels were calculated in reads per kilobase of transcript per million mapped reads (RPKM) using Cufflinks. DEGs were identified with the DESeq2 R package. The thresholds for classification as a DEG in the transgenic lines compared to the WT were $P < 0.05$ and $|\log_2 \text{fold change}| > 1$.

DAP-seq and protein analysis

The full-length coding sequences of *ZmGLK1* and *ZmG2* were amplified from cDNA of the maize accession B73. Each sequence was recombined into the p-rHLO vector using LR Clonase II (Invitrogen). The rHLO *ZmGLK1* and rHLO *ZmG2* proteins were generated using 500 ng each of the p-rHLO *ZmGLK1* and p-rHLO *ZmG2* plasmids DE-squaw

considered significant at $P < 0.05$. Figures were generated with GraphPad Prism 9.0 and Adobe Illustrator CS3.

Accession numbers

Raw sequence data generated in this study have been deposited in the NCB BioProject database under accession number PRJN1018861 for RNA-seq and PRJN1019016 for DTP-seq. The sequence data from this article can be found in the GenBank/EMBL database under the following accession numbers: ZmGLK1 GenBank: F318580 and ZmGLK2 GenBank: F318579.

Acknowledgments

We would like to thank Prof. Jonathan L. Doe from Oxford University for kindly providing the ZmUBI_{pro}:ZmGLK1 and ZmUBI_{pro}:ZmGLK2 rice seeds.

Author contributions

W.Z. and J.L. conceived and designed the experiments. J.L., J.L., S.W., H., and R. performed most of the experiments. Z.L. and R.P. performed the DTP-seq experiment. P.W. critically commented and edited the manuscript. The manuscript was prepared by J.L., J.L., and W.Z. All authors discussed and commented on the manuscript.

Supplemental data

The following materials are available in the online version of this article.

Supplemental Figure S1. Enhanced tolerance of ZmUBI_{pro}:ZmGLK1 and ZmUBI_{pro}:ZmGLK2 rice plants to drought stress induced by 0% PE 6000.

Supplemental Figure S2. Overexpression of ZmGLK1 or ZmGLK2 increased stomatal conductance and photosynthetic parameters in response to drought.

Supplemental Figure S3. Dynamic changes of soil water content during the drought stress in the greenhouse experiment.

Supplemental Figure S4. Genome-wide summary of the regulatory network downstream of ZmGLK1 and ZmGLK2 based on DTP-seq data.

Supplemental Figure S5. Changes in endogenous B content in WT, ZmUBI_{pro}:ZmGLK1, and ZmUBI_{pro}:ZmGLK2 rice leaves under normal conditions and after 7 d of drought stress.

Supplemental Figure S6. Relative expression levels of B biosynthetic genes in the leaves of WT, ZmUBI_{pro}:ZmGLK1, and ZmUBI_{pro}:ZmGLK2 rice plants under normal conditions and after 7 d of drought stress.

Supplemental Table S1. Relative change of gene expression level of 50 overexpressed genes from RNA-seq and DTP-seq analyses.

Supplemental Table S2. Primers used for RT-qPCR.

Funding

This study was supported by grants from the National Key Research and Development Program of China

2016 FD030010. W.Z. was supported by the Innovation Program of the Chinese Academy of Agricultural Sciences and the Elite Youth Program of the Chinese Academy of Agricultural Sciences. J.L. was supported by the National Natural Science Foundation of China 3160137.

Conflict of interest statement. The authors declare that they have no conflict of interests.

Data availability

The data underlying this article are available in the article and its online supplementary material.

References

- Ahmad R, Liu Y, Wang TJ, Meng Q, Yin H, Wang X, Wu Y, Nan N, Liu B, Xu ZY. OLDEN-L: ETR transcription factors regulate WRKY40 expression in response to abscisic acid. *Plant Physiol* 019:179: 1877–1860. <https://doi.org/10.1101/pp.180166>
- Ambavaram MM, Basu S, Krishnan A, Ramegowda V, Batlang U, Rahman L, Baisakh N, Pereira A. Coordination of photosynthesis and rice increases yield and tolerance to environmental stress. *Nat Commun* 019:51:530. <https://doi.org/10.1038/ncomms630>
- Caine RS, Harrison EL, Sloan J, Flis PM, Fischer S, Khan MS, Nguyen PT, Nguyen LT, Gray JE, Croft H. The influences of stomatal density on rice drought stress resilience. *New Phytol* 03:237:6: 1809–1815. <https://doi.org/10.1111/nph.18707>
- Caine RS, Yin XJ, Sloan J, Harrison EL, Mohammed U, Fulton T, Biswal AK, Dionora J, Chatter CC, Coe RA, et al. Rice with reduced stomatal density conserves water and has improved drought tolerance under future climate conditions. *New Phytol* 019:221:1: 371–387. <https://doi.org/10.1111/nph.15377>
- Candido-Sobrinho S, Lima V, Freire F, de Souza L, Gago J, Fernie AR, Daloso DM. Metabolism mediated mechanisms underpin the differential stomatal speediness regulation among ferns and angiosperms. *Plant Cell Environ* 02:45:2: 306–311. <https://doi.org/10.1111/pce.15033>
- Chang YM, Liu WY, Shih ACC, Shen MN, Lu CH, Lu MYJ, Yang HW, Wang TY, Chen SCC, Chen SM, et al. Characterizing regulatory and functional differences between maize mesophyll and bundle sheath cells by transcriptomic analysis. *Plant Physiol* 01:160:1: 165–177. <https://doi.org/10.1101/pp.119203810>
- Chen K, Li GJ, Bressan RA, Song CP, Zhu JK, Zhao Y. Abscisic acid dynamics, signaling, and functions in plants. *J Integr Plant Biol* 2020:62:12:5–57. <https://doi.org/10.1111/jipb.18000>
- Chen M, Ji M, Wen B, Liu L, Li S, Chen X, Gao D, Li L. OLDEN-L: ETR transcription factors of plants. *Front Plant Sci* 016:7:1509. <https://doi.org/10.3389/fpls.016.01509>
- Chen ZH, Chen G, Dai F, Wang Y, Hills A, Ruan YL, Zhang G, Franks PJ, Nevo E, Blatt MR. Molecular evolution of grass stomata. *Trends Plant Sci* 017:22: 117–130. <https://doi.org/10.1016/j.tplants.016.00005>
- FAO. Global agriculture to feed 10 billion: how to feed the world in 2050. Rome: 009.
- FAO 2021. Drought and agriculture. <https://www.fao.org/land-water/drought/drought-and-agriculture/>
- Hall LN, Rossini L, Cribb L, Langdale JA. OLDEN: a novel transcriptional regulator of cellulose differentiation in the maize leaf. *Plant Cell* 1998:10:6: 5–36. <https://doi.org/10.1105/tpc.10.6.5>
- Hsu PK, Dubeaux G, Takahashi Y, Schroeder JI. Signaling mechanisms in abscisic acid-mediated stomatal closure. *Plant J* 01:1:105: 307–311. <https://doi.org/10.1111/j.15067>
- Kim D, Langmead B, Salzberg SL. HISAT: a fast and accurate long-memory requirements. *Nat Methods* 015:12: 357–360. <https://doi.org/10.1038/nmeth.3317>

- Kim TH, Bohmer M, Hu H, Nishimura N, Schroeder JI. Sugar and cell signaling in the regulation of stomatal closure: advances in understanding the molecular mechanisms. *CO₂ and C₃ sugar signaling in plants*. Rev Plant Biol. 2010;61(1):561–591. <https://doi.org/10.1176/plantrev.plantrev.007809.1000.1000.6>
- Kushiro T, Okamoto M, Nakabayashi K, Yamagishi K, Kitamura S, Asami T, Hirai N, Koshiba T, Kamiya Y, Nambara E. The *Arabidopsis* cytochrome P450 CYP707 encodes a 8-hydroxylase: key enzymes in the biosynthesis of salicylic acid. *EMBO J*. 2007;23(7):1657–1666. <https://doi.org/10.1038/s.embo.7600711>
- Landi S, Hausman JF, Guerriero G, Esposito S. Potassium vs. drought stress: focus on drought and salt stress, recent insights and perspectives. *Front Plant Sci*. 2017;8(1):1. <https://doi.org/10.3389/fpls.2017.00001>
- Langmead B, Trapnell C, Pop M, Salzberg SL. Ultrafast and memory-efficient alignment of short DNA sequences to the human genome. *Bioinformatics*. 2009;23(12):1651–1659. <https://doi.org/10.1093/bioinformatics/btp354>
- Lawson T, Viallet-Chabrand S. Speedy stomatal photosynthesis and plant water use efficiency. *New Phytol*. 2010;221(1):93–98. <https://doi.org/10.1111/nph.15330>
- Li X, Wang P, Li J, Wei S, Yan Y, Yang J, Zhao M, Langdale JA, Zhou W. Maize GOLDEN2-LIKE2 encodes a novel protein kinase that regulates photosynthesis and reducing photo-inhibition. *Commun Biol*. 2021;2(1):151. <https://doi.org/10.1038/s43773-020-00887-3>
- Lima VF, Anjos LD, Medeiros DB, Candido-Sobrinho SA, Souza LP, Gago J, Fernie AR, Daloso DM. The sucrose to malate ratio correlates with the faster CO₂ and light stomatal responses of sugarcane compared to ferns. *New Phytol*. 2019;223(4):1873–1887. <https://doi.org/10.1111/nph.15977>
- Liu H, Li X, Xiao J, Wang S. A convenient method for simultaneous quantification of multiple phytohormones and metabolites: application in study of rice abscisic acid interaction. *Plant Methods*. 2018;14(1):1. <https://doi.org/10.1186/s12864-018-4811-8>
- Livak KJ, Schmittgen TD. Analysis of relative gene expression data using real-time quantitative PCR and the $2^{-\Delta\Delta CT}$ method. *Methods*. 2001;25(4):402–408. <https://doi.org/10.1006/meth.2001.2600>
- Magome H, Nomura T, Hanada A, Takeda-Kamiya N, Ohnishi T, Shinma Y, Katsumata T, Kawaide H, Kamiya Y, Yamaguchi S. CYP714B1 and CYP714B2 encode β -glucanase that reduces β -glucanase activity in rice. *Proc Natl Acad Sci USA*. 2013;110(5):1977–1981. <https://doi.org/10.1073/pnas.1215788110>
- Manna M, Thakur T, Chirom O, Mandlik R, Deshmukh R, Salvi P. Transcription factors as key molecular targets to strengthen the drought stress tolerance in plants. *Physiol Plant*. 2011;172(3):877–886. <https://doi.org/10.1111/pp.11368>
- McAusland L, Viallet-Chabrand S, Davey P, Baker NR, Brendel O, Lawson T. Effects of kinetics of light induced stomatal responses on photosynthesis and water use efficiency. *New Phytol*. 2016;211(4):1099–1110. <https://doi.org/10.1111/nph.14000>
- Murmu J, Wilton M, Allard G, Pandeya R, Desveaux D, Singh J, Subramaniam R. *Arabidopsis* OLDEN-L E-L transcription factors activate a smog-like J- dependent disease susceptibility to the biotrophic pathogen *Hyaloperonospora arabidopsidis*, as well as J- independent plant immunity against the necrotrophic pathogen *Botrytis cinerea*. *Mol Plant Pathol*. 2015;15(17):1871–1881. <https://doi.org/10.1111/mpp.12077>
- Nagatoshi Y, Mitsuda N, Hayashi M, Inoue S, Okuma E, Kubo A, Murata Y, Seo M, Saji H, Kinoshita T, et al. OLDEN-L E-L transcription factors for chloroplast development affect drought tolerance through the regulation of stomatal movement. *Proc Natl Acad Sci USA*. 2016;113(15):4181–4186. <https://doi.org/10.1073/pnas.1513031113>
- Nguyen CV, Vrebalov JT, Gapper NE, Zheng Y, Zhong SL, Fei ZJ, Giovannoni JJ. Transcription factors OLDEN-L E-L reveal molecular regulators that function during fruit development and ripening. *Plant Cell*. 2017;29(3):585–601. <https://doi.org/10.1105/pc.113.118777>
- Ozeki K, Miyazawa Y, Sugiura D. Rapid stomatal closure contributes to higher water use efficiency in maize compared to C₃ Poaceae crops. *Plant Physiol*. 2018;178(1):188–203. <https://doi.org/10.1093/plphys/kwz000>
- Pandey S, Zhang W, Assmann SM. Roles of ion channels and transporters in guard cell signaling and stomatal regulation. *FEBS Lett*. 2007;581(1):33–36. <https://doi.org/10.1016/j.febslet.2007.07.008>
- Powell AL, Nguyen CV, Hill T, Cheng KL, Figueroa-Balderas R, Aktas H, Ashrafi H, Pons C, Fernandez-Munoz R, Vicente A, et al. A form of ripening encodes a Golden 2-like transcription factor regulating tomato fruit chloroplast development. *Science*. 2017;356(6398):1711–1715. <https://doi.org/10.1126/science.1252218>
- Ray DK, Mueller ND, West PC, Foley JA. Global trends in sustainable double crop production by 2050. *PLoS One*. 2013;8(6):e66088. <https://doi.org/10.1371/journal.pone.0066088>
- Ray DK, Ramankutty N, Mueller ND, West PC, Foley JA. Recent patterns of crop yield growth and stagnation. *Nat Commun*. 2013;4(1):193. <https://doi.org/10.1038/ncomms2006>
- Rossini L, Cribb L, Martin DJ, Langdale JA. The maize Golden2 gene defines a novel class of transcriptional regulators in plants. *Plant Cell*. 2001;13(5):31–44. <https://doi.org/10.1105/pc.13.5.31>
- Seo M, Koshiba T. Complex regulation of β -glucanase in plants. *Trends Plant Sci*. 2007;12(1):1–8. [https://doi.org/10.1016/S1360-1385\(01\)00187-7](https://doi.org/10.1016/S1360-1385(01)00187-7)
- Sierla M, Hörak H, Overmyer K, Waszczak C, Yarmolinsky D, Maierhofer T, Vainonen JP, Salojärvi J, Penessiouk K, Laanemets K, et al. The receptor-like pseudokinase RLK1 is required for stomatal closure. *Plant Cell*. 2018;30(11):813–837. <https://doi.org/10.1105/pc.18.00771>
- Tang Y, Li M, Chen Y, Wu P, Wu G, Jiang H. Knockdown of OsPAO and OsRCCR1 cause different plant development phenotypes in rice. *J Plant Physiol*. 2011;168(16):1095–1105. <https://doi.org/10.1016/j.plaphy.2011.05.006>
- Tilman D, Balzer C, Hill J, Befort BL. Global food demand and the sustainable intensification of agriculture. *Proc Natl Acad Sci USA*. 2011;108(50):4560–4564. <https://doi.org/10.1073/pnas.1110737108>
- Todaka D, Nakashima K, Shinozaki K, Yamaguchi-Shinozaki K. To understand the transcriptional regulatory networks in drought stress responses and tolerance in rice. *Rece*. 2015;1(6). <https://doi.org/10.1186/1939-8333-5-6>
- Wang F, Liu J, Chen